

4 Design of the UHV-SQUID system

One aim of this PhD-thesis was the setup of an ultrahigh vacuum (UHV)-chamber for ultrathin magnetic film analysis comprising a SQUID-magnetometer to determine the magnetization of a sample on an absolute scale. In this chapter the construction of the UHV-system and the design and calibration of the SQUID is described. Magnetic, structural and chemical investigations are exemplarily demonstrated for ultrathin Fe films grown on a Cu(100) and a GaAs(001) single crystals, respectively. First SQUID measurements are presented confirming the functionality of the system. The UHV-setup offers the opportunity to perform SQUID and ferromagnetic resonance (FMR) [40] measurements on the *same* sample for the first time.

4.1 Construction of the UHV chamber

The UHV-chamber (welded by the company VTS Schwarz [179]) is designed on the basis of a sphere of 150 mm radius. All main flanges are focussed on the center of the sphere. The principle axes x , y , z are used as follows:

- x -axis: sample manipulation; glass finger for FMR measurements (magneto-optical Kerr effect (MOKE) possible).
- y -axis: Low energy electron diffraction (LEED) for structural investigation and Auger electron spectroscopy (AES) for chemical analysis and film thickness determination.
- z -axis: sample preparation by electron beam evaporation from below and SQUID magnetometry from above.

Moreover, the following devices are incorporated in the UHV-chamber:

- Sputter gun for sample cleaning with Ar^+ -ions.
- Quadrupol mass spectrometer for residual gas analysis.
- Rotatable aperture plate used during evaporation to create thin films of an area of 3×3 mm².
- Plasma gun for controlled reactive gas exposure (O, H, N atoms and ions).

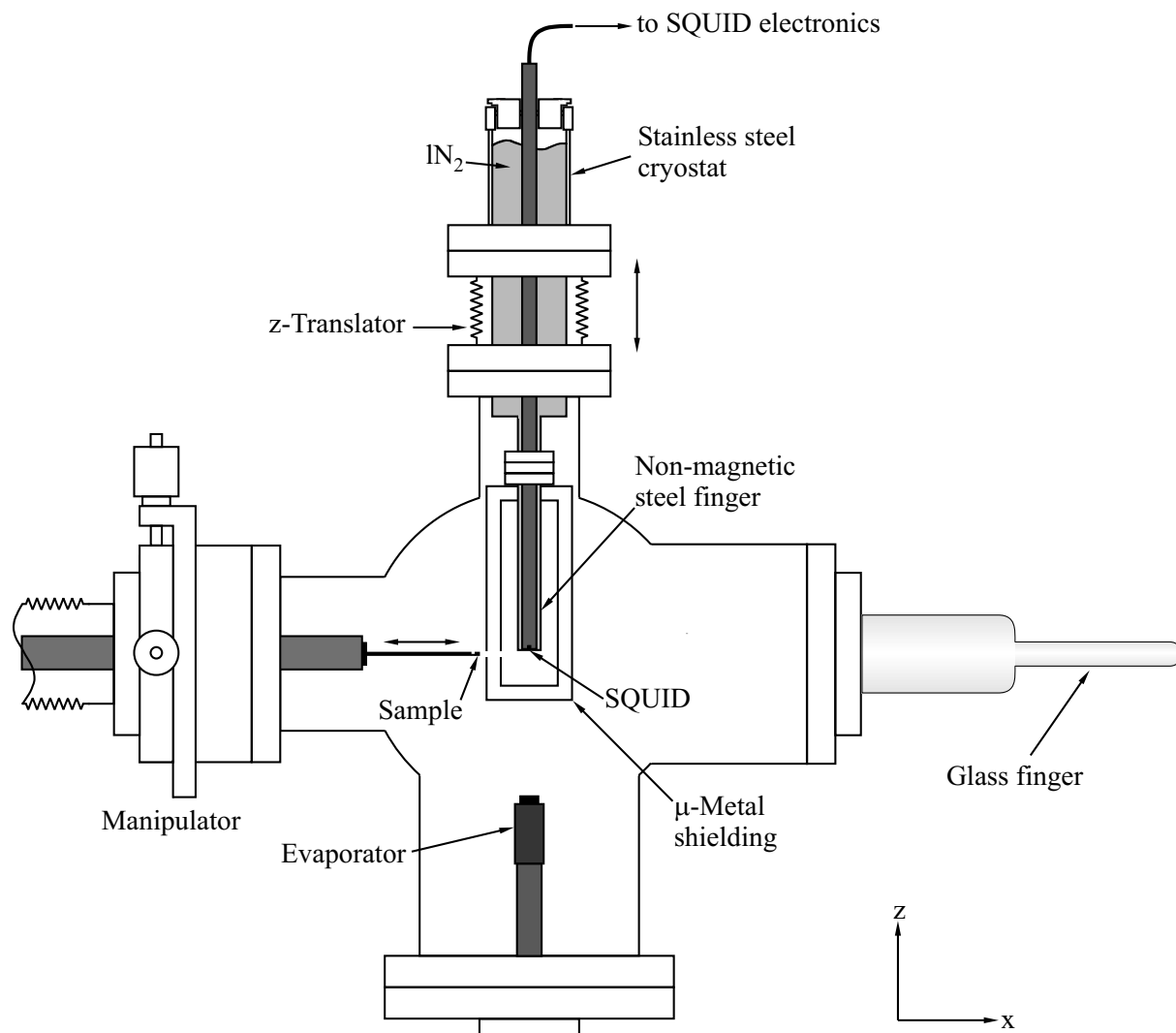


Figure 4.1: UHV-SQUID setup. Square-shaped ferromagnetic films of $3 \times 3 \text{ mm}^2$ can be evaporated by means of an aperture plate. Before SQUID measurements the sample is magnetized in the tip of the glass finger by an external field along the x - or the z -axis, then the SQUID setup including the LN_2 -cryostat and the double wall μ -metal screening is vertically transferred to the center of the chamber. At a distance of $\approx 4 \text{ mm}$ the sample is moved laterally to the SQUID in order to measure its magnetic stray field. The LEED optics and the cylindrical mirror analyzer for structural characterization and Auger-spectroscopy, respectively, are directed along the y -axis through the center of the spherical chamber (not shown).

- Rotary vane pump, turbo molecular pump (250 l) and ion getter pump (300 l) and Titanium sublimation pump (TSP).
- Longauge for UHV pressure measurement.
- One main viewport (DN 63 CF) and several smaller ones (DN 38 CF, DN 16 CF).

The complete list of the flange positions and a technical drawing of the chamber is given in the appendix (table A.3 and Fig. A.1). A simplified cross section through the x - z -plane of the

UHV-chamber is shown in Fig. 4.1. An ultrathin film sample, e. g. Fe/Cu(100), which has been grown by electron beam evaporation is transferred to the tip of the glass finger where an external field is applied in order to magnetize the sample to a single domain out-of-plane or in-plane state. At a distance of ≈ 4 mm the sample is then moved laterally to the SQUID which resides in a μ -metal shielded, liquid nitrogen (LN_2) filled non-magnetic metal dewar. From the detected magnetic stray field as described in chapter 2.3.2 the magnetization of the thin film is determined on an absolute scale. The base pressure is on the order of 2×10^{-8} Pa.

4.2 The SQUID sensor

The high- T_c rf-SQUID sensor M900 used in this work is a standard sensor of the JSQ company [180]. It is made out of YBCO deposited on a SrTiO_3 substrate with the Josephson junction fabricated by pattern induced grain boundaries. The technical data of the sensor are listed in the appendix (table A.4). The rod which incorporates the SQUID has been custom-made, in order to suit the dimensions of the finger of the metal cryostat. A drawing of its dimensions can be found in the appendix A.4 (a).

4.3 Cryostat and magnetic shielding

The UHV-compatible LN_2 -cryostat is mounted vertically to the chamber and consists of two parts: the upper part accounting for $\approx 90\%$ of the volume and the non-magnetic metal finger mounted thereunder. In order to minimize the thickness of the bottom of the cryostat a non-magnetic sheeting of 0.5 mm was used for the finger tip. The SQUID sensor is kept *ex situ* under LN_2 in close vicinity to the bottom resulting in a distance to the sample of ≈ 4 mm. As demonstrated in Fig. 2.10 a reduction of the distance between SQUID and sample tremendously increases the detected signal.

Both the cryostat and the magnetic shielding stand temperatures in the range of 77 K (LN_2 -cooling) to 500 K during the baking procedure. The SQUID, however, is removed before baking the system and is warmed up with dry air, since the sensor stands neither temperatures above 350 K nor water, which condensates on the SQUID rod after the use in LN_2 if the rod is not warmed up.

The cryostat is manufactured of a single stainless steel tube of 0.3 mm wall thickness, which is thermally isolated by the ultrahigh vacuum within the chamber. In order to avoid mechanical vibrations the thin-walled tube is supported by an outer stainless steel tube of 2 mm thickness, which simultaneously acts as a radiation shield. Lateral oscillations are inhibited, whereas an axial expansion during baking and contraction under LN_2 is possible. The support tube is welded on a DN CF 63-flange and welded to the inner tube via a metal ring of 1 mm, which reduces

the thermal conduction to the chamber. Additionally, the cryostat is encapsulated by a closely matching Polyoxymethylene cap at the feed opening, which prevents the vessel from icing up during the utilization of liquid nitrogen. At the bottom of the inner tube a DN 16 CF-flange is welded to which the non-magnetic metal finger is mounted. The dimensions of the cryostat are given in Fig. A.4 (b) of the appendix. In order to shield the cryostat finger against magnetic fields it is surrounded by a double wall μ -metal cylinder. The accurate dimensions of this construction are depicted in Fig. A.3.

4.4 The sample holder

The sample holder is solely fabricated of non-magnetic materials in order to allow for detecting only the stray field of the ferromagnetic film grown on the Cu- or GaAs-single crystal. The holder is made of one piece of oxygen-free copper (OFHC) for the purpose of optimum thermal conduction during cooling with liquid helium. Annealing of the sample is achieved via resistive heating using a W-wire of 0.3 mm thickness, which is plugged through two bores within the crystal. Since the sample is transferred horizontally during SQUID measurements the crystal has to be adequately stabilized mechanically to suppress vibrations of the W-wire. To impede an overheating of the whole sample holder during annealing up to 900 K ceramic tubes of 0.8 mm² connect the crystal with the holder in a distance of 3 mm, which simultaneously fix the substrate. Moreover, ceramic tubes of different sizes are used to isolate the non-magnetic *Pallaplat*¹ thermocouple, which is used for temperature control, and the electrical wiring as depicted in Fig. 4.2. In order to use the sample holder as an electric conductor it is isolated

¹The *Pallaplat* 32/40 thermocouple consists of 95% Pt 5% Rh / 52% Au 46% Pd 2% Pt.

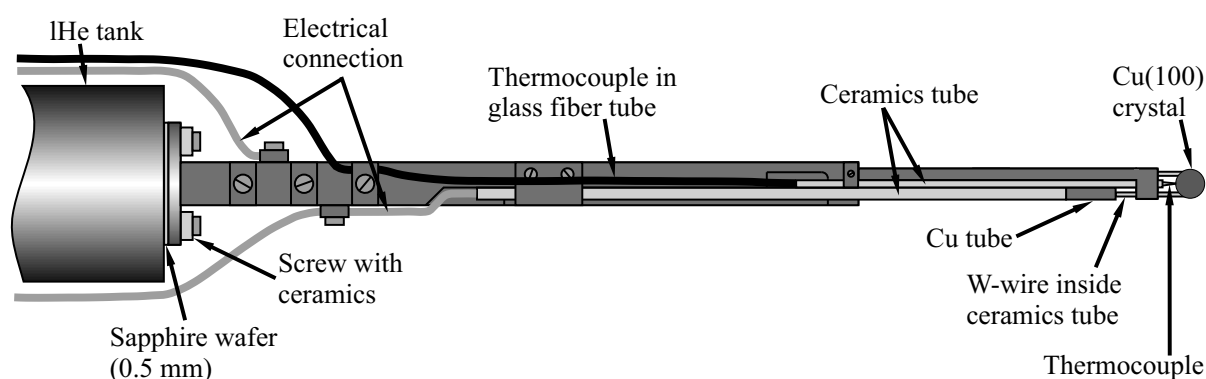


Figure 4.2: Top view of the non-magnetic sample holder made of oxygen-free copper, which is connected to the IHe-cooled manipulator via a sapphire plate. The substrate is held by a tungsten wire of 0.3 mm thickness for resistive heating, guided by two ceramic tubes of 0.8 mm outer diameter (gray), which stabilize the crystal (dark gray). The sample holder and the electrical connections are isolated from ground potential via a sapphire wafer of 0.5 mm thickness.

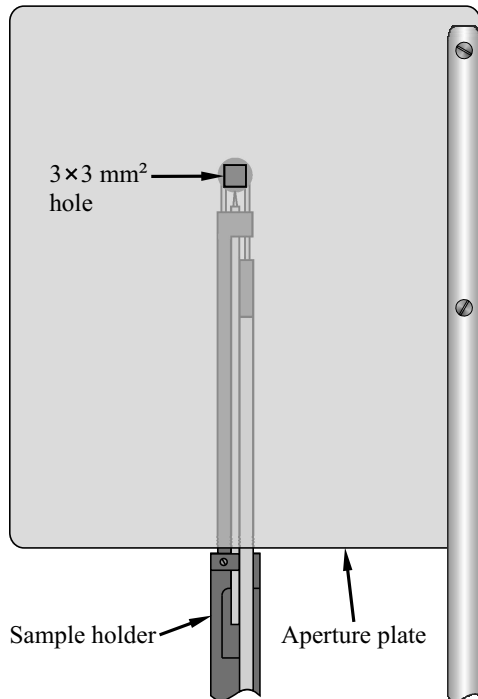


Figure 4.3: By means of the aperture plate ferromagnetic films of $3 \times 3 \text{ mm}^2$ size are grown on the single crystal substrate. The dimensions of the aperture plate are chosen, such that the whole part of the sample holder, which enters the magnetic shielding, is covered during evaporation. This ensures that the stray field measured by SQUID exclusively originates from the grown film. After evaporation the aperture can be rotated off its position.

from the manipulator, which is on ground potential, by a sapphire wafer which ensures a good thermal conduction during cooling. One end of the W-wire is directly screwed to the sample holder by a molybdenum slug, while the other end is connected to a Cu-wire by a Cu-tube crimping the ends of the wires.

In order to evaporate an ultrathin magnetic film of rectangular shape² onto the single crystal substrate, an aperture plate with a square-shaped hole of $3 \times 3 \text{ mm}^2$ is used as shown in Fig. 4.3. Keeping the distance between the substrate surface and the aperture plate below $\approx 0.5 \text{ mm}$, an ultrathin film is evaporated through the hole onto the substrate. The distance between the evaporator and the substrate is 130 mm , therefore the film is of the same size as the hole of the aperture. Fig. 4.3 also shows that the whole part of the sample holder, which enters the μ -metal shielding, is covered by the aperture plate³ during the evaporation. This is necessary in order to protect the holder from contamination by ferromagnetic materials. Thus, it is ensured that the stray field measured by SQUID exclusively originates from the grown film.

4.5 Calibration of the SQUID

The magnetic flux which crosses the area of the SQUID loop is detected, and it is converted by the electronics into an output voltage proportional to the magnetic field perpendicular to the loop. A determination of the magnetic field component on an absolute scale, however, requires

²Only the stray field component B_z of rectangular films can be simulated by the Eqs. (2.12) and (2.13).

³The width and the length of the aperture plate are 66 mm and 75 mm , respectively.

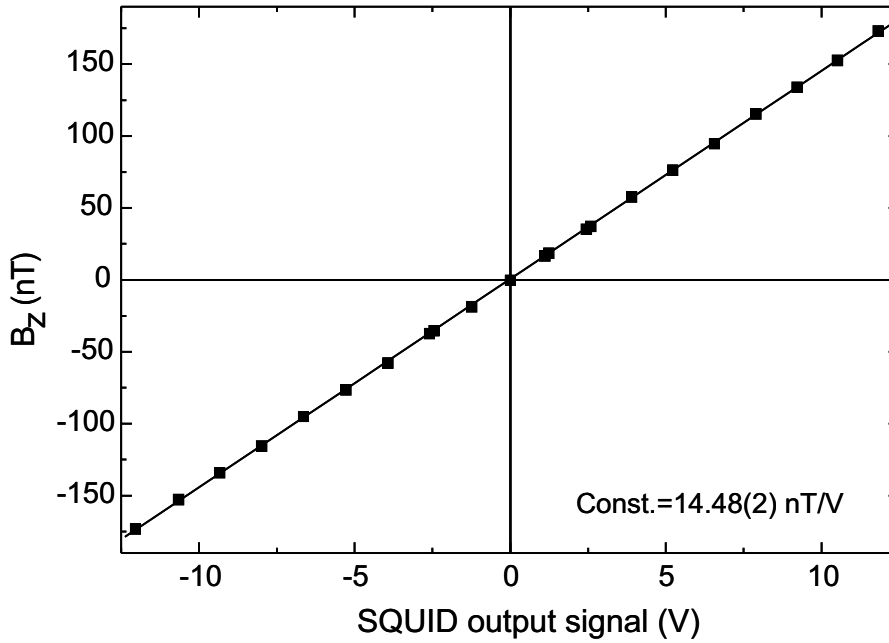


Figure 4.4: Calibration of the SQUID sensor signal by means of a small coil. The calibration factor yields 14.48(2) nT/V.

a calibration of the SQUID. The SQUID has a factory adjusted field-to-flux ratio setting of $9.3 \text{ nT}/\Phi_0$. The transfer coefficient of the electronics was adjusted to a high voltage-to-flux ratio of $0.64(1) \text{ V}/\Phi_0$ by means of an oscilloscope, using the triangle pattern in the test mode of the SQUID. Both settings in combination yield the desired field-to-voltage ratio $14.5(2) \text{ nT/V}$. A much more precise method, which is necessary in order to determine the magnetic moments per atom of a single monolayer of a ferromagnetic material, is the calibration by the magnetic field of a small current conducting loop. Since the SQUID is a $100 \mu\text{m} \times 100 \mu\text{m}$ ring in the center of the sensor head, a small calibration coil ($r = 6.5 \text{ mm}$) of two turns is sufficient to create an almost homogeneous magnetic field in the SQUID. Within an *ex situ* setup described elsewhere [181], which consists of a non-magnetic cryostat and a double μ -metal shielding, a high-precision current in the μA -range was applied to a Cu-coil around the SQUID sensor. The sensor resided in the center of the coil, which had a radius of $r = 6.75 \text{ mm}$ and two turns n . The resulting current (I) depending magnetic field B at the site of the SQUID is given by:

$$B = \mu_0 I \frac{n}{2r} \quad (4.1)$$

with $\mu_0 = 1.2566 \times 10^{-6} \text{ VsA}^{-1}\text{m}^{-1}$ and yields for the used coil $B = 0.186(7) \cdot \text{nT}/\mu\text{A}$. The calibration factor arising from this method is given by the slope of the linear fit in Fig.4.4, which is $14.48(2) \text{ nT/V}$ in excellent agreement with the previous determination but with higher accuracy.

4.6 Data acquisition

The magnetized sample is moved laterally below the SQUID sensor as sketched in Fig. 4.1 by the use of a motor-driven manipulator. In order to minimize the vibrations the motor is driven continuously. The setting parameters like the measuring velocity, the number and length of single scans and the data acquisition are controlled by the same computer program. By means of an AD-DA transformer card the output voltage of the SQUID is assigned to the actual motor position. Since the SQUID signal is proportional to the perpendicular component of the sample's stray field according to the calibration curve shown in Fig. 4.4 the stray field distribution as a function of the x -position is obtained. A detailed description of the operation of the program and the performance of the measurements can be found in the appendix A.3.

4.7 Measurements of the stray field of a 12.5 ML Fe/GaAs(001) film

In order to test the UHV-SQUID magnetometer, an ultrathin Fe film of 12.5 ML thickness was grown on a GaAs(001) single crystal surface. The Fe layer thickness was determined by using a quartz micro balance. The expected layer thickness based on the previously determined calibration curve of the Fe evaporator (see Fig. A.7) was 10 ML. Since Fe was evaporated on a semiconductor substrate, a thickness determination via Auger electron spectroscopy as described for the case of Fe/Cu(100) in section 3.2 was not possible.

Before the stray field measurements our sample was in-plane magnetized by an external magnetic field of ≈ 8 kA/m along the x -direction, which is the scan direction (see Fig. 4.1) and parallel to the $[0\bar{1}1]$ axis of the crystal. The easy axis of the magnetization is parallel to the scan direction. In Fig. 4.5 three different SQUID measurements of the 12.5 ML Fe/GaAs(001) film are superposed. The stray field component B_z (nT)⁴ is shown versus the x -position (mm). No data smoothing has been performed. The inset in the figure reveals an average noise of ≈ 0.4 nT. Within this noise the measurements are reproducible. The peak-to-peak signal is about 20 nT, so that the resulting signal-to-noise ratio is about 50 : 1. The limiting signal-to-noise ratio is assumed to be 3 : 1. Moreover, the measured signal scales linearly with respect to the film thickness and the magnetization. Therefore, the sensitivity limit is ≈ 0.6 ML of Fe in the present configuration of the UHV-SQUID system. However, as the asymmetric shape of the stray field distribution reveals, there are still some problems with the setup, since in the ideal case (see section 2.3.2) a homogeneously magnetized film should give rise to a symmetric curve. The sources of error are discussed in the following, and they have to be solved in order to determine the magnetization of an ultrathin film on an absolute scale in future experiments. The

⁴The SQUID output voltage is converted into nT by the calibration coefficient.

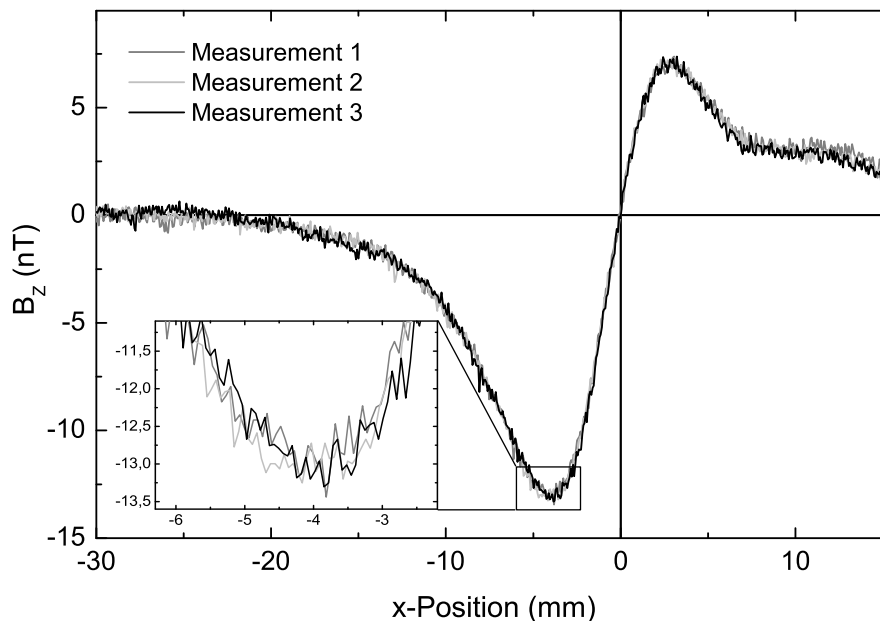


Figure 4.5: Measured stray field component B_z of a 12.5 ML Fe/GaAs(001) film, which was in-plane magnetized along the x -direction. The three different measurements at 300 K are reproducible within an average noise level of 0.4 nT. The signal-to-noise ratio is about 50:1. The asymmetric shape of the curves is attributed to both a tilt of the sample and a ferromagnetic signal originating from the sample holder.

sample holder, which is composed of non-magnetic materials only, obviously contains traces of ferromagnetic substances. This is indicated by the shoulder on the right hand side of the stray field curve, which is unlikely to originate from the Fe film. Therefore, a measurement of the sample holder and the blank substrate is indispensable. The main source of the asymmetric shape of the curves, however, is attributed to a tilt of the sample with respect to the z -axis of the UHV system (see Fig. 4.1). This tilt causes a linear variation of the distance between the SQUID and the sample during the scanning process, which was shown in section 2.3.2 to strongly influence the measured signal.

In conclusion, with the present calibrated UHV-SQUID setup the stray field distribution $B_z(x)$ of an in-plane magnetized ultrathin film can be reproducibly detected on an absolute scale with a high signal-to-noise ratio. In order to determine the magnetization from simulations of the measured stray field, however, further improvements of the system have to be done.